LABORATORI NAZIONALI DI FRASCATI
SIS – Pubblicazioni

LNF-96/015 (P)
18 Marzo 1996

Effects of Higher–Coordination Shells in Garnets Detected by XAS at the Al K–edge

Ziyu Wu[1,2], Augusto Marcelli[1], Annibale Mottana[3], Gabriele Giuli[4,5], Eleonora Paris[5], and Friedrich Seifert[6]

[1]INFN – Laboratori Nazionali di Frascati, P.O. Box 13, I–00044 Frascati (Italy)

[2]Institut des Matériaux de Nantes, CNRS UMR 110, Laboratoire de Chimie des Solides, 2 Rue Houssinière, 44072 Nantes Cedex 03, (France)

[3]Dipartimento di Scienze Geologiche, Università di Roma III Via Ostiense 169, I–00154 Roma (Italy)

[4]Dottorato in Mineralogia e Petrologia, Università di Firenze, I–50121 Firenze, (Italy)

[5]Dipartimento di Scienza della Terra, Università di Camerino, I–62032 Camerino (Italy)

[6]Bayerisches Geoinstitut, Univeristät Bayreuth, D–95440 Bayreuth (Germany)

Abstract

The aluminium 1s x–ray–absorptionspectra of a series of garnets, pyrope ($Mg_3Al_2Si_3O_2$), almandine ($Fe_3Al_2Si_3O_{12}$), spessartine ($Mn_3Al_2Si_3O_{12}$) and grossular ($Ca_3Al_2Si_3O_{12}$), are compared to full multiple–scattering calculations using cluster models. An overall good agreement between experiment and calculation, extended also to the edge region, is obtained in the energy range up to 60 eV above the threshold, provided clusters containing at least 40 atoms are used. The analysis of these garnet XAS spectra provides clear evidence on the effect of atoms located far away from the first–coordination shell around the photoabsorber. As a local probe, XANES spectroscopy at the edge of low Z elements appears to be a perfect tool to investigate the role played by atoms located in higher–coordination shells.

PACS.: 78.70.Dm. 75.50.Pp, 91.60.Pn, 91.35.Lj

Submitted to Phys. Rev. B Rapid Commun.

Recently, increased attention has been focused on x-ray absorption spectroscopy (XAS) as a powerful tool for structural analysis and for studying the electronic properties around the selected atom, because of the success achieved by the full multiple-scattering (MS) theory in explaining near-edge features[1,2] and because of the forefront experimental results at the K-edge of low Z atoms obtained by using new monochromators[3–5] or novel crystals as YB_{66}[6]. Here, we present a series of theoretical and experimental results for the Al K-edge x-ray absorption near-edge structure (XANES) spectra of pyrope (Pyr), almandine (Alm), spessartine (Sps) and grossular (Grs) garnets, and show how the MS theory requires contributions arising from atoms located in higher-coordination shells to explain the observed features.

Garnets are important not only for their physical properties[7], but also for being the rock-forming minerals best suited to establish the pressure conditions of crustal metamorphics and Upper Mantle rocks.

The general structural formula of cubic garnets can be expressed as $X_3Y_2Z_3O_{12}$[8], where X = Mg, Fe, Mn, Ca within eight-fold coordinated dodecahedra, Y = Al, Fe, Cr with octahedral coordination (in this study Y refers to Al), and Z = Si with tetrahedral coordination. The unit-cell parameters and the atomic clusters up to the third shell around the photoabsorbing Al atom are shown in Table 1. Note that the unit-cell of a garnet in the $Ia3d$ space group comprises 96 O, 16 Y, 24 Z and 24 X atoms, i.e., all together, a cluster of 160 atoms extending to about 7 Å from the center.

The experimental data were collected at the Stanford Synchrotron Radiation Laboratory (SSRL), using the JUMBO monochromator equipped with YB_{66} crystals. Spectra acquisition was typically from 1540 to 1690 eV at 0.5 eV intervals, and with 7 s counting times. The resolution of YB_{66} at 1550 eV is 0.46 eV[9].

Figure 1 shows the experimental Al K-edge XANES spectra after background subtraction for our four garnets. The general shape of these XANES spectra is qualitatively similar because garnets have all the same crystal structure. Close inspection of Figure 1, however,

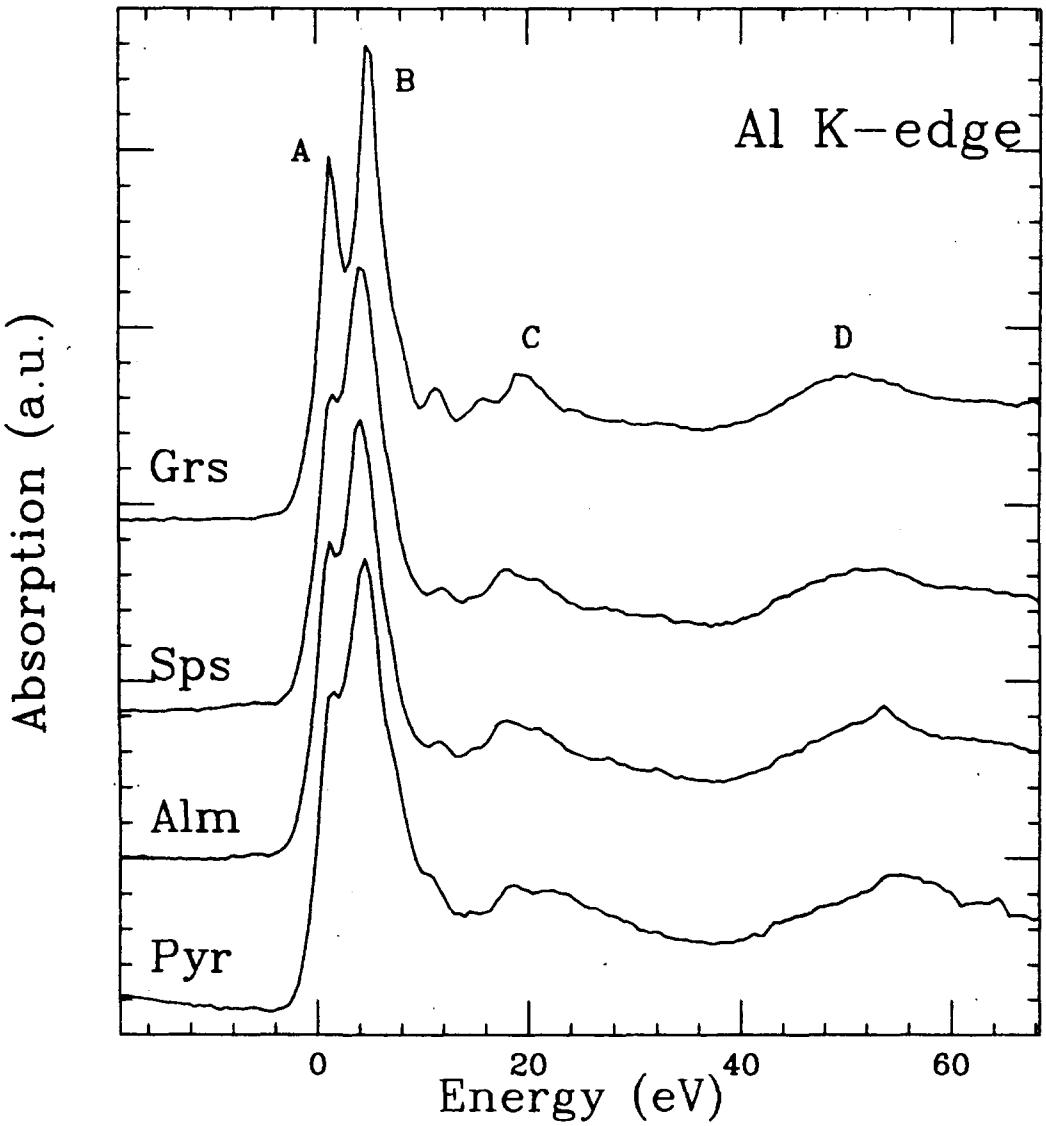

Fig. 1. Experimental Al K-edge XANES spectra for pyrope (Pyr, $Mg_3Al_2Si_3O_{12}$), almandine (Alm, $Fe_3Al_2Si_3O_{12}$), spessartine (Sps, $Mn_3Al_2Si_3O_{12}$) and grossular (Grs, $Ca_3Al_2Si_3O_{12}$).

shows several features, labelled A to D, which behave differently among the four samples. For example, peak A increases, and peaks C and D shift toward lower energies in moving from Pyr to Alm, Sps, and Grs. These features are located both at the threshold and in the MS region. An interpretation of their origin will certainly clarify the local atomic arrangement around the Al site of these garnets.

The XANES spectra have been computed on the basis of the MS theory[1,10–19] using the CONTINUUM code[20]. In the muffin-tin model and one-electron approximation, local density potential for the system can be constructed based on Mattheiss' prescription[21], by superposition of neutral atomic charge densities using the Clementi-Roetti's basis set tables[22]. For the exchange-correlation part of the potential we have tested two different types of approach: energy-independence of the X_α, and the energy- and position-dependent complex Hedin-Lundqvist (H-L) self-energy $\Sigma(\vec{r}, E)$[23]. In order to simulate the charge relaxation around the core hole in a photoabsorber of atomic number Z (13 in the case of Al), we used the well screened $Z+1$ approximation (final state rule)[12]. This consists in taking the orbitals of the $Z+1$ atom and constructing the charge density by using the excited electronic configuration of the photoabsorber with the core electron promoted to an empty orbital. We have chosen the muffin-tin radii according to Norman's criterion[24], and allowed a 10% overlap between contiguous spheres to simulate the atomic bond. The consequent solution of the effective Schrödinger equation for final state is solved numerically. The unpolarized photoabsorption cross section σ for photons with energy ω, in Rydberg units of energy and lengths, is given by[17]

$$\sigma(\omega) = 2\frac{4\pi^2}{3}\alpha\omega \sum_{L,m_\gamma,m_0} |< \Psi^-_{kL}|[\frac{4\pi}{3}]^{1/2} r Y_{lm_\gamma}|\Psi_{L_0}>|^2 \qquad (1)$$

where $\Psi^-_{kL}=(\Psi^+_{kL})^*$ is the time-reversed scattering wave function in response to an exciting free wave of angular momentum $L=(l,m)$ and Ψ_{L_0} is a core-state, usually $1s, 2s, 2p, ..$; moreover r is the dipolar operator and Y_{lm_γ} are the spherical harmonics. The exponential 2 results from the spin degrees of freedom and $k=\sqrt{E}$, E being the photoelectron kinetic energy. The calculated spectra are further convoluted with a Lorentzian shaped function

with a full width Γ_h[25,26] to account for the core hole lifetime and Γ_{exp}, the experimental resolution.

In Figure 2 we present theoretical calculations of the Al K-edge XANES spectra for pyrope (left panel) and grossular (right panel), respectively, by using clusters of different size around the excited Al atom. The first coordination shell, consisting of six O atoms, already gives rise to a relatively sharp peak, labelled *B*, that shift to lower energy just after introducing some additional coordination spheres in the cluster used for calculation. Alternatively, in terms of scattering process, this structure may be associated to a caging effect, mainly due to the first O shell, on the excited electron: the back-scattering creates a

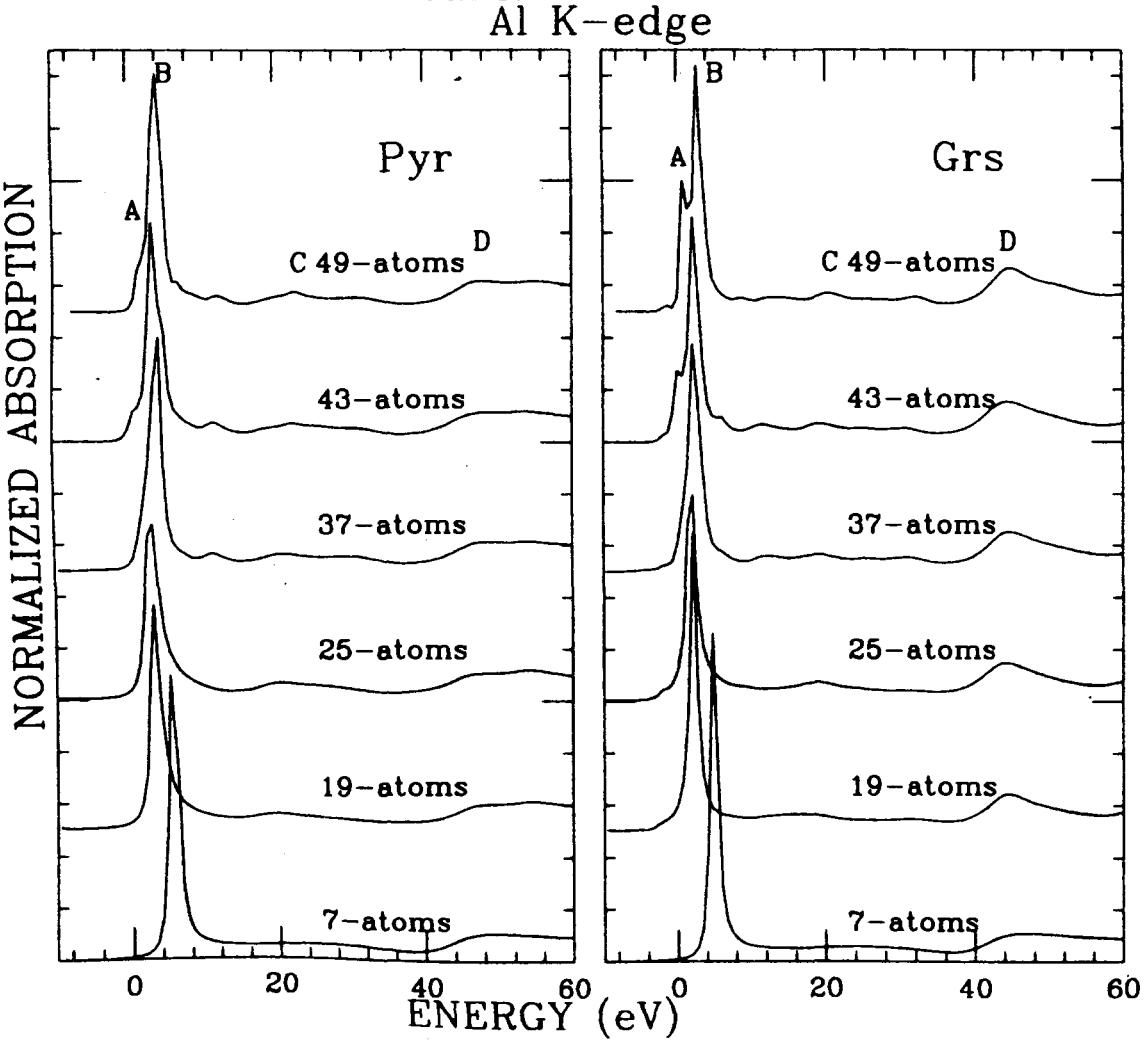

Fig. 2. Theoretical XANES spectra at the Al K-edge as function of the cluster size for pyrope (left panel) and grossular (right panel).

relatively sharp scattering resonance around the absorber atom. This is in agreement with several findings, e.g., on NiO[27], MgO[28,29], and MnO[30].

In the Al K-edge, actually, peak *B* should be attributed to transitions from 1*s* to unoccupied *p*-like states. At treshold, another feature is observed: peak *A*. This peak changes as a function of the *X* atom, its intensity decreasing on going from Ca (Grs) to Mg (Pyr). This behaviour can be then associated with the different electronic configuration of garnets. In particular, peak *A* mainly results from transitions towards Al 3*p* empty states mixed with the empty density of states of the *X* atom (Mg, Fe, Mn and Ca)[31,32]. Peak *A* is reproduced only in calculations with clusters including the fourth and fifth shell around the Al atom, i.e., for Grs, a 49-atom cluster whith 36 O + 6 Si + 6 Ca atoms; for Pyr, the same cluster with 36 O + 6 Si + 6 Mg atoms. This result confirms that the final state reached in the core transitions is not really a simple atomic or molecular state, but it has to be sensitive to long-range effects too[33]. Feature *C* arises approximately when considering contributions of atoms from the second shell (Si and *X* atoms), and involves inter-shell multiple scattering, while peak *D* is reproduced already when using the O first-coordination shell, and arises mainly from dominantly single-scattering events from this shell.

In order to compare the experimental data with our calculations, we present in Figure 3 the four different Al K-edge XANES calculations for Pyr, Alm, Sps, and Grs, respectively, obtained with convergent clusters, i.e., clusters large enough so that spectra calculated for them do not change when adding farther shells. All spectra display the mentioned main features, *A* to *D*, and are in very good agreement with the experimental data shown in Figure 1. As it can be seen, there are two significant trends in the spectra: (i) the relative amplitude of peak *A* increases monotonically from Pyr to Grs; and (ii) the energy positions of peaks *C* and *D* shift negatively in the same order, albeit slightly.

In the structure of each of these garnets, the Al atom is octahedrally surrounded by oxygen, at distances which are 1.88 Å for Pyr[8], 1.89 Å for Alm[8], 1.90 Å for Sps[34], and 1.92 Å for Grs[34]. The next-nearest neighbours are Si and Mg at 3.20 Å for Pyr, Si and Fe at 3.22

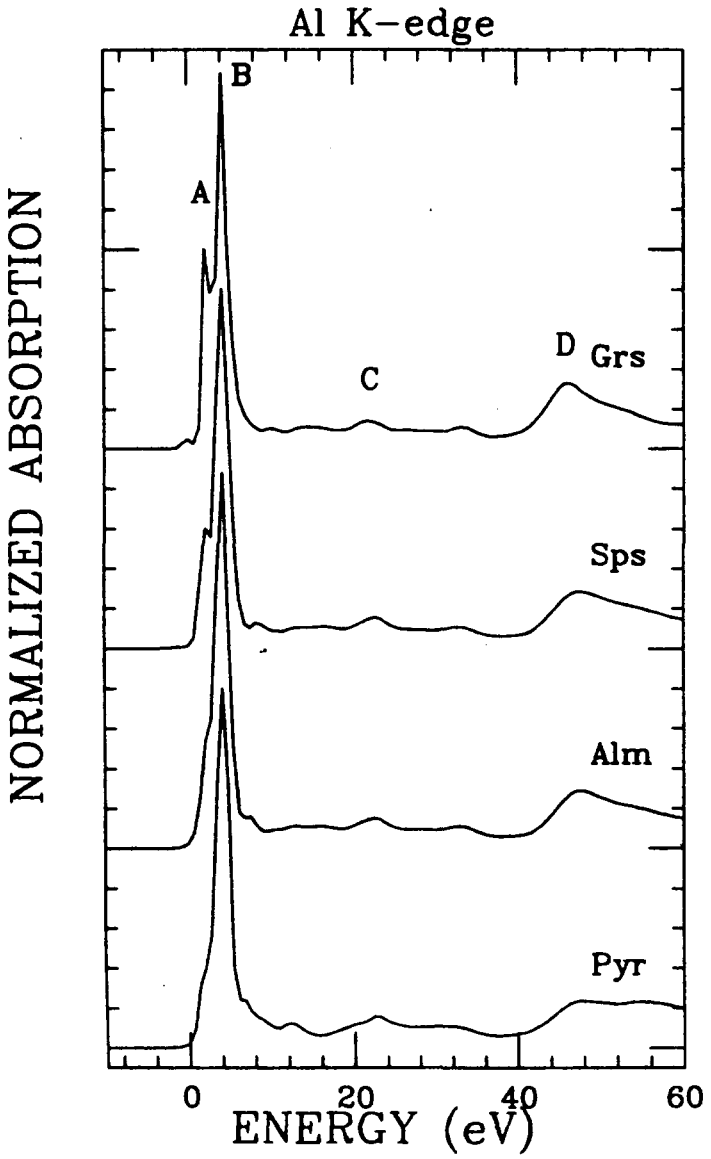

Fig. 3. MS calculations of the Al K-edge XANES of the four garnets reported in Figure 1, obtained with clusters of the same size.

Å for Alm, Si and Mn at 3.24 Å for Sps, and Si and Ca at 3.31 Å for Grs, respectively, as shown in Table 1.

Table 1. The cubic unit-cell edge and the nearest Al-O and Al-X (X = Mg, Fe, Mn, Ca) shell distances (in Å) of the four garnets.

Sample	$Mg_3Al_2Si_3O_{12}$[a]	$Fe_3Al_2Si_3O_{12}$[a]	$Mn_3Al_2Si_3O_{12}$[b]	$Ca_3Al_2Si_3O_{12}$[b]
a_0	11.452	11.525	11.612	11.845
⟨Al-O⟩	1.8857×6	1.8904×6	1.9008×6	1.9242×6
⟨Al-Si⟩	3.2009×6	3.2213×6	3.2457×6	3.3108×6
⟨Al-Mg⟩	3.2009×6	-	-	-
⟨Al-Fe⟩	-	3.2213×6	-	-
⟨Al-Mn⟩	-	-	3.2457×6	-
⟨Al-Ca⟩	-	-	-	3.3108×6

[a] Ref.[8]

[b] Ref.[34]

As noted above, we associate the behaviour of peak *A* to the increase of the unoccupied states, in particular of 3*d* character, available to atoms located in higher-coordination shells for mixing with the Al states[35,36]. Indeed, the number of unoccupied 3*d* states decreases from Ca to Fe to Mn (Mg has no 3*d* states), following the same trend observed in the garnet series (i.e., Grs to Alm to Sps). Thus, the higher-energy features *C* and *D* could be interpreted using the well-known relation that links the energy position of the resonance peak at threshold (i.e., *B*) with the distance (R) between the excited atom and the back-scattering cage[37]:

$$\Delta E R^2 = const. \qquad (2)$$

This equation holds true in our case because the different potentials can be realistically assumed to be similar, and also because the expected variation of interatomic distances is

well-contained, being the relative variation less than 10%: thus, the two basic assumptions backing the equation are met. The presence of features which basically scale with interatomic distances (Table 1) is a clear demonstration of the presence in these Al XAS spectra of contributions from higher-order coordination shells or, in other words, of a significant influence of the atoms surrounding the Al absorber, other than oxygen, on the electronic properties of Al itself.

The calculations shown in Figure 2 confirm that peak D reflects resonance scattering from the six O first-nearest-neighbours around Al. However, peak C starts being reproduced only after adding the second shell (Si and X atoms at 3.2-3.3 Å). Nevertheless, both our calculations and the experimental data, in different ways, show that peak C actually sits in a region of the spectrum rich of several other minor features; a further, more accurate analysis is advisable that may discriminate contributions associated with distortions inside the first coordination shells from those due to the higher-coordination ones.

During our MS calculations we have found that the H-L exchange-correlation potential does not give any significant improvement over X_α; however we have included no figures reporting the results of these calculations. The complex part of it produces an excessive electron damping, in such a way that features lying between B and D nearly desappear. This reflects the established fact that the X_α potential is probably the best for certain insulating materials.

In conclusion, we carried out a detailed experimental and theoretical investigation of the Al K-edge XANES spectra of four natural garnets: pyrope ($Mg_3Al_2Si_3O_{12}$), almandine ($Fe_3Al_2Si_3O_{12}$), spessartine ($Mn_3Al_2Si_3O_{12}$) and grossular ($Ca_3Al_2Si_3O_{12}$). We have obtained a very good agreement between experimental data and one-electron full MS calculations of the Al K-edges of these compounds. Our comparison, starting from a simplified resonance scattering model,

(i) relates the variation in intensity of the pre-peaks with the electronic properties of the system, i.e., the local character of the partial empty density of states; and

(ii) discusses, and in some cases identifies, other observed features as being the scattering resonances arising from the first-, second-, and higher-order shells. However, additional work is required to improve the latter description.

Indeed, within the full MS theory reference framework, both single-scattering (SS) and multiple-scattering (MS) processes are assumed to contribute to a spectrum, although SS contributions from shells of neighbouring atoms (EXAFS-like) are expected to be more intense than the MS ones. The significant signals observed in ordered structures come from both these processes; thus, the interpretation of the specific features of the garnet spectra which lie at energies between 5 and 60 eV above the threshold requires the accurate simulation of all SS and MS paths in large atomic clusters. Neverthless, these preliminary results on garnets show that this method can be extented to other similar materials or to structurally complex compounds and/or to disorder systems. Work is in progress to improve the simulation, and to extend the analysis to other natural and synthetic garnets.

ACKNOWLEDGMENTS

This work was supported by a Human Capital and Mobility EC grant (ZYW) and by a M.U.R.S.T. project (AM). Experiments (proposal No. 2317) were done at SSRL, which is operated by the Department of Energy, Office of Basic Energy Science. Thanks are due to Joe Wong, Michael Rowen and the entire SSRL staff for continuous assistance.

REFERENCES

1. P.J. Durham, in: *X – ray Absorption : Principles, Applications, Techniques of EXAFS, SEXAFS, XANES*, eds. R. Prinz and D. Koningsberger (Wiley, New York, 1988).

2. *Proceedings of the 8th International Conference on X – ray Absorption Fine Structure*, Berlin 1994, eds. K. Baberschke, and D. Arvanitis, North-Holland.

3. C.T. Chen, and F. Sette, Rev. Sci. Instrum. **60**, 1616 (1989).

4. Z. Hussain, E. Umbach, D.A. Shirley, J. Stohr, and J. Feldhaus, Nucl. Instr. Meth. **195**, 115 (1982).

5. T. Murata, T. Matsukava, S. Naoè, and O. Matsudo, Rev. Sci. Instrum. **60**, 2128 (1989).

6. J. Wong, G.N. George, I.J. Pickering, Z.U. Rek, M. Rowen, T. Tanaka, G.H. Via, B. De Vries, D.E.W. Vaughan, and G.E. Brown Jr., Solid State Commun. **92**, 559 (1994).

7. S. Geller, in: *Proceedings of International School of Physics E. Fermi*, Course LXX, (Varenna, 1977, North Holland, 1978) p. 1.

8. T. Armbruster, C.A. Geiger, and G.A. Lager, American Mineralogist **77**, 512 (1992).

9. M. Rowen (priv. commun., 1995).

10. *Core – level spectroscopy in condensed systems*, eds. J. Kanamori and A. Kotani (Springer-Verlag, New York, 1988).

11. P.A. Lee, and J.B. Pendry, Phys. Rev. **B 11**, 2795 (1975).

12. P.A. Lee, and G. Beni, Phys. Rev. **B 15**, 2862 (1977).

13. C.R. Natoli, D.K. Misemer, S. Doniach, and F.W. Kutzler, Phys. Rev. **A 22**, 1104 (1980).

14. P.J. Durham, J.B. Pendry, and C.H. Hodges, Comput. Phys. Commun. **25**, 193 (1982).

15. C.R. Natoli, and M. Benfatto, J. Phys. (Paris) Colloq. **47**, C8-11 (1986).

16. C.R. Natoli, M. Benfatto, and S. Doniach, Phys. Rev. **B 34**, 4682 (1986).

17. C.R. Natoli, M. Benfatto, C. Brouder, M.Z. Ruiz Lopez, and D.L. Foulis, Phys. Rev. **B 42**, 1944 (1990).

18. Z.Y. Wu, M. Benfatto, and C.R. Natoli, Phys. Rev. **B 45**, 531 (1992), and Z.Y. Wu, M. Benfatto, and C.R. Natoli, Solid State Commun. **87**, 475 (1993).

19. T.A. Tyson, K.O. Hodgson, C.R. Natoli, and M. Benfatto, Phys. Rev. **B 46**, 5997 (1992) and references therein.

20. C.R. Natoli (unpublished).

21. L. Mattheiss, Phys. Rev. **A 134**, 970 (1964).

22. E. Clementi, and C. Roetti, *Atomic Data and Nuclear Data Tables*, **Vol. 14**, (1974).

23. H. Chou, J.J. Rehr, E.A. Stern, and E.R. Davidson, Phys. Rev. **B 35**, 2604 (1987) and references therein.

24. J.G. Norman, Mol. Phys. **81**, 1191 (1974).

25. J. Chem. Ref. Data **8**, 2 (1979).

26. J.C. Fuggle, and J.E. Inglesfield, *Unoccupied Electronic States*, Topics in Applied Physics (Berlin: Springer) (1992); Appendix B p. 347.

27. D.D. Vvedensky, and J.B. Pendry, Phys. Rev. Lett. **54**, 2725(1985).

28. Th. Lindner, H. Sauer, W. Engel, and K. Kambe, Phys. Rev. **B 33**, 22 (1986).

29. P. Rez, X. Weng, and H. Ma, Microsc. Microanal. Microstruct. **2**, 143 (1991).

30. H. Kurata, E. Lefevre, C. Cilliex, and R. Brydson, Phys. Rev. **B 47**, 13763 (1993).

31. D. Li, G.M. Bancroft, M. Kasrai, M.E. Fleet, X.H. Feng, K.H. Tan, and B.X. Yang,

Solid State Commun., **87**, 613 (1993).

32. D. Li, G.M. Bancroft, M.E. Fleet, X.H. Feng, and Y. Pan, American Mineralogist, **80**, 432 (1995).

33. A.V. Soldatov, T.S. Ivanchenko, S. Della Longa, A. Kotani, Y. Iwamoto, and A. Bianconi, Phys. Rev. **B 50**, 5074 (1994).

34. G.A. Novak, and G.V. Gibbs, American Mineralogist **56**, 791 (1971).

35. F.M.F. de Groot, M. Grioni, J.C. Fuggle, J. Ghijsen, G.A. Sawatzky, and H. Petersen, Phys. Rev. **B 40**, 5715 (1989).

36. Z.Y. Wu, G. Ouvrard, P. Gressier, and C.R. Natoli, to be published.

37. C.R. Natoli, Springer Series Chem. Phys. **27**, 43 (1983).